Original article

MOLECULAR METABOLISM

CD73 promotes the immunoregulatory functions of hepatic Tregs through enzymatic and nonenzymatic pathways in MASLD development

Hua Jin[1,2,3,7], Xinjie Zhong[1,2,7], Chunpan Zhang[4,7], Yongle Wu[2,7], Jie Sun[1,2], Xiyu Wang[1,2], Zeyu Wang[1,2], Jingjing Zhu[1,2], Yuan Jiang[1,2], Xiaonan Du[1,2,3], Zihan Zhang[1,2,3], Dong Zhang[1,2,5], Guangyong Sun[1,2,6,*]

ABSTRACT

Metabolic dysfunction-associated steatotic liver disease (MASLD) is a leading chronic liver disease characterized by chronic inflammation. Regulatory T cells (Tregs) highly express CD73 and play a critical role in modulating the immune response. However, the roles and mechanisms by which CD73 modulates Tregs in MASLD are still unknown. A choline-deficient high-fat diet (CDHFD) or methionine/choline-deficient diet (MCD) was used to establish a MASLD model. We found that CD73 expression was upregulated in Tregs via the FFA-mediated p38/GATA2 signaling pathway. *Cd73* KO promoted MASLD progression, accompanied by decreased Treg viability and activity. Compared with *Cd73* KO Tregs, adoptively transferred WT Tregs exhibited increased Treg activity and provided greater protection against hepatic inflammatory responses in MASLD. This immune protection is mediated by CD73 via both enzymatic and nonenzymatic pathways, degrading AMP into ADO to increase Treg function and block DR5-TRAIL-mediated cell death signaling. These findings suggest a potential immunotherapeutic approach for MASLD treatment and highlight its possible relevance for clinical application.

Keywords CD73; Regulatory T cells; Metabolic dysfunction-associated steatotic liver disease; Adenosine; TRAIL

1. INTRODUCTION

Metabolic dysfunction-associated steatotic liver disease (MASLD) is one of the most important causes of liver disease worldwide and is likely to become a major cause of end-stage liver disease in the coming decades [1]. MASLD involves the accumulation of intrahepatic triglycerides (simple steatosis), intrahepatic steatosis, inflammatory changes, and varying degrees of hepatocellular injury (metabolic dysfunction-associated steatohepatitis, MASH) and eventually progresses to liver fibrosis, cirrhosis, and hepatocellular carcinoma (HCC) [2,3]. In most patients with MASLD, liver histology is characterized by simple steatosis, whereas up to 50% of patients exhibit inflammation and/or fibrosis [3]. Patients with MASLD, especially those with MASH or liver fibrosis, suffer from long-term complications that lead to increased mortality [4].

MASLD can be affected by many factors, such as metabolic factors, drugs and environmental factors [5]. As a key metabolic organ in the body, the liver regulates energy and lipid metabolism and has a strong immune functions [6]. MASLD is characterized by chronic low-grade inflammation in the liver [7], caused by an imbalance of proinflammatory and anti-inflammatory factors between innate immune cells and adaptive immune cells in the body [8]. In the immune system, a special $CD4^+$ T-cell population, namely, regulatory T cells (Tregs), plays an important role in maintaining immune homeostasis in the liver [9]. Tregs inhibit the activation and proliferation of $CD4^+$ and $CD8^+$ T cells and suppress the secretion of inflammatory factors and cytotoxicity to maintain peripheral immune tolerance and control immune responses under pathological and physiological conditions [10,11]. Previous studies have shown that oxidative stress mediates Treg apoptosis and leads to the loss of Tregs in the steatotic liver, which in turn activates the TNF-α signaling pathway, increases liver inflammation, and causes simple steatosis and further liver injury [12,13]. However, the specific mechanism by which Tregs regulate the intrahepatic immune microenvironment and prevent MASLD needs to be further studied.

Tregs highly express CD73 (ecto-5′-nucleotidase) and CD39, and CD73/CD39-mediated purinergic signaling plays a critical role in the suppressive properties of Tregs [14]. CD73 is an important ectonucleotidase that catalyzes the conversion of extracellular adenosine

[1]Medical Research Center, Beijing Institute of Respiratory Medicine and Beijing Chao-Yang Hospital, Capital Medical University, Beijing 100020, China [2]Department of Gastroenterology, Beijing Chao-Yang Hospital, Capital Medical University, Beijing 100020, China [3]Immunology Research Center for Oral and Systemic Health, Beijing Friendship Hospital, Capital Medical University, Beijing 100050, China [4]Department of Infectious Diseases, Beijing Friendship Hospital, Capital Medical University, Beijing 100050, China [5]Beijing Laboratory of Oral Health, Capital Medical University School of Basic Medicine, Beijing 100069, China [6]General Surgery Department, Beijing Friendship Hospital, Capital Medical University, Beijing 100050, China

[7] Hua Jin, Xinjie Zhong, Chunpan Zhang, and Yongle Wu contributed equally to this work.

*Corresponding author. Medical Research Center, Beijing Institute of Respiratory Medicine and Beijing Chao-Yang Hospital, Capital Medical University, Beijing 100020, China. E-mail: sungy@ccmu.edu.cn (G. Sun).

Received October 1, 2024 • Revision received March 17, 2025 • Accepted March 20, 2025 • Available online 24 March 2025

https://doi.org/10.1016/j.molmet.2025.102131

monophosphate (AMP) to adenosine (ADO) [15]. Many studies have shown that Tregs in adipose tissue regulate the development of obesity through the HIF-1α-Med23-PPAR-γ axis [16]. CD73 also plays an important role in regulating lipid droplet transport and adipocyte differentiation [17]. However, it is unclear how CD73 affects the intrahepatic immune microenvironment by regulating Tregs in the MASLD liver, especially in this special fatty acid environment.

In this study, we found that CD73 expression on Tregs was upregulated in the livers of individuals with MASLD, which inhibited the intrahepatic proinflammatory environment by regulating the survival and immunomodulatory function of Tregs and alleviating the pathogenesis of MASLD. Mechanistically, free fatty acids (FFAs) in the liver upregulate the expression of CD73 on Tregs through p38 and the transcription factor GATA2. CD73 affects the survival and immunoregulatory function of Tregs through enzymatic and nonenzymatic pathways in MASLD livers with abnormal lipid metabolism. The findings of the present study provide new targets and therapeutic strategies for the prevention and treatment of MASLD.

2. MATERIALS AND METHODS

2.1. Animals

Eight-week-old weight-matched male wild-type (WT) C57BL/6 mice were purchased from Beijing Vital River Laboratory (Beijing, China). Male C57BL/6 *Cd73* knockout (KO) (stock no. 018986), Foxp3^{GFP+} transgenic (stock no. 023800), C57BL/6-GFP (stock no. 004353), and *Rag1* KO (stock no. 002216) mice were purchased from The Jackson Laboratory (Bar Harbor, ME, USA). WT mice were divided randomly and fed a normal control diet (NCD), a choline-deficient and ethionine-supplemented diet (CDE, Research Diets, New Brunswick, NJ, USA), a western diet (WD, Research Diets), a methionine/choline-deficient diet (MCD, Beijing HFK Bioscience), or a choline-deficient high-fat diet (CDHFD, Research Diets) to establish the MASLD model. The mice were maintained in a pathogen-free, temperature-controlled (room temperature: 22 ± 2 °C) environment under a 12-hour light/dark cycle at Beijing Friendship Hospital, and all the animal protocols were approved by the Institutional Animal Care and Ethics Committee (No. 20-2042).

2.2. Isolation of liver immune cells via enzymatic digestion

After anesthesia, the liver was perfused with normal saline (NS) until it appeared pale. The liver was subsequently excised and chopped into small pieces, followed by dissociation with a gentle-MACS Dissociator and further digestion in 0.01% type IV collagenase for 30 min at 37 °C. The cell suspension was filtered through a 70-μm cell strainer, and liver immune cells were purified via 33% Percoll density gradient centrifugation as previously described [18]. Purified immune cells in liver samples were stained and detected via fluorescence-activated cell sorting (FACS) with an Aria II system (BD Biosciences, CA, USA). The data were analyzed via FlowJo software (Treestar, Ashland, OR, USA).

2.3. Adoptive transfer experiments

CD3$^+$ T cells (5 × 10^6) from the spleen and lymphoid tissue of male WT mice were transferred into sex-matched *Rag1* KO mice via tail vein injection to establish a W/WT Treg-transferred model. CD3$^+$ T cells without CD4$^+$CD25$^+$CD127$^-$ T cells (Tregs) were also transferred into *Rag1* KO mice to establish a W/O Treg-transferred model. In addition, CD3$^+$ T cells without Tregs from WT mice and Tregs from *Cd73* KO mice were mixed at a ratio of 10:1 and adoptively transferred to *Rag1* KO mice to establish a W/*Cd73* KO Treg-transferred model. The above recipient mice and control *Rag1*$^{-/-}$ mice not subjected to cell transfer were subsequently fed an MCD for 4 weeks, after which MASLD development was estimated.

2.4. Histology and immunohistochemistry

Liver tissues from the mice were fixed, dehydrated, embedded in paraffin, and cut into 5 μm sections. Hematoxylin and eosin (H&E) staining and Oil Red O staining were performed via Servicebio Technology (Wuhan, China). Activated hepatic stellate cells were assessed via immunohistochemistry with a pAb against α-smooth muscle actin (α-SMA) (Servicebio). Three experienced liver pathologists, with no prior knowledge of the experimental groups, were blinded during the analysis of the NAS scores (based on steatosis, inflammation, and ballooning) for H&E staining of liver sections from the mice, Oil Red O-positive areas, and α-SMA-positive areas.

2.5. Enzyme-linked immunosorbent assay (ELISA)

Mouse TNF-α (EK0527), IFN-γ (EK0375), IL-1β (EK0394), and IL-6 (EK0411) ELISA kits were purchased from BOSTER Biological Technology Co., and the cytokine levels in plasma were detected according to the manufacturer's protocols.

2.6. Reagents and antibodies

Fluorochrome-conjugated antibodies against mouse CD45 (clone 30-F11), CD11b (clone M1/70), F4/80 (clone BM8), Ly6G (clone 1A8-Ly6g), CD3 (clone 145-2C11), CD4 (clone GK1.5), CD8 (clone 53—6.7), TNF-α (clone MP6-XT22), IFN-γ (clone XMG1.2), IL-17 (clone TC11-18H10.1), CD25 (clone 3C7), CD127 (clone A7R34), FOXP3 (clone MF-14), Ki67 (clone 16A8), Granzyme B (clone QA16A02), CTLA4 (clone UC10—4B9), Tim-3 (B8.2C12), IL-10 (clone JES5-16E3), CD69 (clone H1.2F3), DR5 (clone MD5-1), Perforin (clone S16009A), TGF-β1 (clone TW7-16B4), and CD73 (clone TY/11.8) were obtained from BioLegend; antibodies against human CD3 (clone SK7), CD4 (clone A161A1), CD25 (clone BC96), CD127 (clone A019D5), and CD73 (clone AD2) were purchased from BioLegend. An Annexin V-PE kit (640908; BD Biosciences), a Caspase-3 staining kit (C1168M; Beyotime Biotechnology, China), antibodies against B-cell lymphoma 2 (BCL-2; 3498; CST), and B-cell lymphoma-extra large (BCL-XL; 2767; CST) were used to evaluate cell survival. Alanine aminotransferase (ALT), aspartate aminotransferase (AST), and total bilirubin (TBIL) detection kits were purchased from Nanjing JianCheng Biochemical Institute (China).

2.7. Treg and monocyte isolation

Tregs were obtained from the splenocytes of WT or *Cd73*—KO mice via a MojoSort™ Mouse Regulatory T-Cell isolation kit (480137; Biolegend). Tregs were cultured with complete medium consisting of RPMI-1640 supplemented with 10% fetal bovine serum, 1% penicillin-streptomycin, and 2 mM L-glutamine in 96-well plates with an anti-mouse CD3 antibody (3 μg/ml; 100238; Biolegend) and an anti-mouse CD28 antibody (1 μg/ml; 102116; Biolegend) at 37 °C with 5% CO2.

Monocytes were collected from the bone marrow of C57BL/6 mice, and erythrocytes were lysed after cell filtration with a 70-μm cell strainer. Gr1$^+$, B220$^+$, and Ter119$^+$ cells were removed via magnetic column selection, and purified monocytes were obtained from the remaining cells. Next, monocytes were cultured in complete medium supplemented with 20 ng/ml M-CSF for 5 days in 6-well plates and incubated with or without 100 ng/ml LPS for an additional 12 h.

2.8. *In vitro* coculture assay

Tregs ($CD3^+NK1.1^-CD4^+CD8^-CD25^+CD127^-$ subsets) from the livers of MCD-fed WT and *Cd73* KO mice were sorted via flow cytometry. $CD3^+$ T cells from C57BL/6-GFP mice were obtained from the spleens via mouse T-cell enrichment columns. $CD3^{GFP+}$ T cells were cultured with or without Tregs at a ratio of 4:1 in 96-well plates with an anti-mouse CD3/CD28 antibody. After 3 days, the apoptosis and proliferation of the $CD3^{GFP+}$ T cells were detected via flow cytometry.

2.9. *In vitro* stimulation assay with Tregs

FFAs (200 μM) were prepared by mixing oleic acid (O1008; Sigma) and palmitic acid (P0500; Sigma) at a ratio of 2:1 as previously described [19]. FFAs with or without 100 ng/ml recombinant mouse TRAIL protein (1121-TL; R&D) were added to Tregs for 48 h. Tregs were also incubated with 500 ng/ml of recombinant mouse CD73 protein (4488-EN; R&D) or control IgG for 6 h, followed by treatment with 200 μM FFAs and 100 ng/ml of recombinant mouse TRAIL protein for another 48 h.

ATP (A6419; Sigma—Aldrich), AMP (A9396; Sigma—Aldrich), or adenosine (ADO) (A4036; Sigma—Aldrich) was separately added to Tregs from WT or *Cd73* KO mice for 24 h.

For the experiments with inhibitors, Tregs were separately incubated with 10 μM of the p38 inhibitor SB203580 (HY-10256; MCE), 2.5 μM of the AKT inhibitor MK2206 (HY-10358; MCE), 10 μM of the ERK1/2 inhibitor PD98059 (HY-12028; MCE), or 15 μM of the GATA2 inhibitor K-7174 (HY-12743; MCE) for 1 h and then stimulated with 200 μM FFAs for another 48 h.

2.10. Measurement of ATP, AMP, and ADO concentrations

The serum from peripheral blood or culture supernatant was collected to determine the concentrations of ATP, AMP, and ADO. An Enhanced ATP Assay Kit (S0027; Beyotime, China), AMP Assay Kit (LE-M1602; Lai Er Biotech, China), and Adenosine Assay Kit (ab211094; Abcam) were used to determine the concentrations of ATP, AMP, and ADO, respectively, according to the manufacturers' instructions.

2.11. Real-time PCR

TRIzol™ reagent (Sigma—Aldrich, USA) was used to extract total RNA, and PrimeScript™ RT Master Mix (TaKaRa, Japan) was used for reverse transcription into cDNA. Real-time PCR assays were performed via an ABI QuantStudio 3 system (Applied Biosystems, USA). The amplification of each sample represents the relative expression level compared with *Gapdh* expression, and gene expression was quantified via the $2^{-\Delta\Delta Ct}$ method. The primers used in the present study are listed in Supplementary Table 1.

2.12. Transcriptome sequencing analysis

A total of 1×10^4 Tregs ($CD3^+NK1.1^-CD4^+CD8^-CD25^+CD127^-$ subsets) in the livers of WT and *Cd73* KO mice fed a NCD or MCD were sorted via flow cytometry. Each group included 2-3 biological replicates. Total RNA was extracted, and transcriptome sequencing libraries were generated using the Illumina®'s NEBNext® Ultra™ RNA Library Preparation Kit (NEB, USA) and sequenced on the Illumina HiSeq platform (Illumina, San Diego, CA). Differentially expressed genes (DEGs) in Tregs between MCD- and NCD-fed WT mice or between MCD-fed WT and *Cd73* KO mice were identified using the DESeq2 package and defined as those with an absolute fold change $\geq$1.5 and a P value < 0.05. The DEGs were subsequently subjected to Gene Ontology (GO) and Kyoto Encyclopedia of Genes and Genomes (KEGG) enrichment analyses. The mRNA sequencing data described in this study were uploaded to the Gene Expression Omnibus (GEO) database of the National Center for Biotechnology Information (NCBI).

2.13. CUT&Tag assay

Tregs were stimulated with or without 200 μM FFAs for 48 h and sorted to obtain 100,000 live cells for the CUT&Tag assay. The GATA2 antibody (2B5A1; Proteintech) or control IgG antibody, Hyperactive Universal CUT & Tag Assay Kit (TD903-01, Vazyme), and TruePrep Index Kit V2 (TD202; Vazyme) were used to extract the GATA2 binding site and amplify the cDNA libraries. The libraries were subsequently sequenced by Berry Genomics.

2.14. Single-cell RNA sequencing analysis

We analyzed single-cell data from the GEO database, including data from CDHFD-fed mouse liver cells (GSE232182), MCD-fed mouse liver nonparenchymal cells (GSE166178), and WD-fed mouse liver $CD45^+$ lymphocytes (GSE156059). For the GSE156059 dataset, we used "Liver $CD45^+$ cells derived from mice fed a WD for 24 weeks" as the experimental group (WD) and "Liver $CD45^+$ cells derived from mice fed a standard diet for 24 weeks" as the control group (NCD). The raw single-cell sequencing data were processed using R (version 4.3.0) and the Seurat V5 package. After quality control filtering, dimensionality reduction was performed using PCA, followed by UMAP visualization. Tregs were identified based on the coexpression of canonical markers including *Cd3d, Cd3e, Cd3g, Cd4*, and *Foxp3*. We analyzed the expression of *Cd73* (*Nt5e*) on Tregs in CDHFD, MCD, and WD groups. For GSE156059 dataset, the Treg population was further stratified into *Cd73* $(Nt5e)^+$ and *Cd73*$^-$ subsets. DEG analysis between *Cd73*$^+$ and *Cd73*$^-$ Tregs was performed using Wilcoxon rank-sum test, with significance thresholds set at adjusted P value < 0.05 and $|\log2FC| > 0.26$. The functional implications of the differentially expressed genes were assessed through GO enrichment analysis using the clusterProfiler R package.

2.15. Clinical study

The study involved 21 MASLD patients from Beijing Chao-yang Hospital who met the MASLD definition [20]. Twenty patients visiting the Physical Examination Center of Beijing Chao-yang Hospital for routine physical examinations served as healthy controls. The demographic and clinical characteristics of the patients are shown in Supplementary Table 2. Healthy subjects were required to be nondiabetic and free of major organ disease, chronic inflammatory conditions, cancer, active psychiatric diseases, and surgical history. Plasma was collected in vacutainer tubes, and ALT, AST, cholesterol, TBIL, HDL, LDL, and TG levels were measured via standard laboratory techniques. All the subjects provided written informed consent to participate in the study, and the study protocol was approved by the Human Institutional Review Board of Beijing Chao-yang Hospital (No. 2024-ke-380).

2.16. Statistical analysis

Statistical analyses were conducted using Prism 10.0 software (GraphPad Software, USA). The normality of variables was assessed via the Shapiro—Wilk test. For normally distributed and homoscedastic data, comparisons between two groups were performed using the unpaired two-tailed t-test. For datasets fulfilling both normality and homogeneity of variance assumptions, multiple comparisons were analyzed using one-way/two-way ANOVA with Sidak's test as recommended by GraphPad Prism 10.0. For normally distributed but heteroscedastic data, we performed Welch's ANOVA followed by Tamhane's T2 test. For non-normally distributed data, differences were compared using the Kruskal—Wallis test followed by Dunn's test

for multigroup comparisons. A two-sided *P*-value <0.05 was considered statistically significant ($^{*}P < 0.05$; $^{**}P < 0.01$).

3. RESULTS

3.1. CD73 expression on Tregs is increased during MASLD progression

To explore CD73 variation during MASLD development, we established a MASLD mouse model by feeding C57BL/6 mice a CDE diet for 16 weeks, an MCD for 4 weeks, a CDHFD for 16 weeks, or a WD for 24 weeks. As shown in Figure S1A, the *Nt5e* (encoding CD73) mRNA level significantly increased after 16 weeks of the CDE diet. Similarly, compared with that in the livers of the mice fed a NCD, the expression of *Nt5e* in the livers of the MCD-, CDHFD- and WD-fed mice was significantly greater (Figure 1A, B and Fig. S1B). Next, we separated liver cell suspensions into mononuclear cells (MNCs) and hepatocytes, and found that *Nt5e* expression was elevated in MNCs but not hepatocytes in MCD- and CDHFD-fed mice (Figure 1C,D).

To determine which immune cells altered CD73 expression in MASLD, we further assessed the expression of CD73 on immune cells. A typical flow cytometry gating strategy was utilized to distinguish the different immune cells (Fig. S1C). Compared with that in the control mice, CD73 expression was elevated on $CD4^+$ T cells in the peripheral blood and liver of the MCD- and CDHFD-fed mice but not on $CD8^+$ T cells, natural killer (NK) cells, neutrophils, monocytes, or Kupffer cells (Figure 1E—H). A typical flow cytometry gating strategy used to distinguish Tregs is also shown in Figure S1C. According to previous reports [21,22], the $CD4^+CD25^+CD127^-$ subset is a good surrogate for $FOXP3^+$ Tregs. We revealed that the $CD4^+CD25^+CD127^-$ phenotype was strongly correlated with FOXP3 in the liver and spleen of $Foxp3^{GFP+}$ transgenic mice (Fig. S1D). Since FOXP3 staining can reduce cellular viability, we also defined Tregs as $CD4^+CD25^+CD127^-$ T cells to adoptively transfer live Tregs, and detected the Treg survival rate and mRNA levels. Further analysis revealed that Tregs ($CD4^+CD25^+CD127^-$ T cells) highly expressed CD73 and that CD73 expression was markedly elevated in Tregs in both the liver and peripheral blood of MCD- and CDHFD-fed mice (Figure 1I—K). To confirm this result, we also labeled Tregs with FOXP3 antibody, and the ratio and CD73 expression of $FOXP3^+$ Tregs were increased in CDHFD-fed mice, which is similar to the results of Tregs with $CD4^+CD25^+CD127^-$ labeling (Fig. S1E and S1F). In addition, an increase in CD73 expression in the Foxp3-GFP^+ Tregs of the CDHFD- and MCD-fed mice was also validated using $Foxp3^{GFP+}$ transgenic mice (Fig. S1G and S1H). We analyzed data from the GEO public databases (GSE232182 and GSE166178) and confirmed that the expression of *Nt5e* in intrahepatic Tregs of the CDHFD and MCD models was greater than that in the NCD groups (Fig. S1I). Similarly, increased soluble CD73 was also detected in the blood of the mice with MASLD (Fig. 1L).

The $CD4^+$ population of Tregs in human PBMCs expresses high levels of CD25 and low levels of CD127, and the majority of $CD4^+CD25^+CD127^-$ subsets are $FOXP3^+$ cells, suggesting that a combination of CD4, CD25, and CD127 could represent a highly purified population of Tregs in human PBMCs [23,24]. Therefore, we also measured CD73 expression in human Tregs ($CD4^+CD25^+CD127^-$) (Fig. S1J). We collected peripheral blood mononuclear cells (PBMCs) and plasma from 21 MASLD patients and 20 healthy controls. Notably, increased levels of CD73 in Tregs and soluble CD73 in plasma were detected in MASLD patients (Fig. 1M). Furthermore, both the proportion of $CD73^+$ Tregs and the soluble CD73 content were inversely correlated with ALT and AST levels in MASLD patients (Supplementary Table 3), suggesting that CD73 on Tregs might have a key effect on the progression of MASLD.

3.2. *Cd73* knockout decreases intrahepatic Treg survival and immunomodulatory activity and promotes MASLD progression

To elucidate the role of CD73 in MASLD, we fed WT and *Cd73* KO mice a CDHFD or MCD. The *Cd73* KO mice gained markedly more weight than the age-matched WT mice did (Figure 2A). After 16 weeks of CDHFD feeding, the *Cd73* KO mice presented significantly increased plasma levels of ALT, AST, and TBIL (Fig. 2B). Similarly, fasting glucose levels were greater in the CDHFD-fed *Cd73* KO mice than WT mice (Fig. 2C). H&E, Oil Red O and α-SMA staining revealed greater fat accumulation in the livers of the *Cd73* KO mice than in those of the WT mice, accompanied by increased hepatocellular ballooning, histological signs of lobular inflammation and focal liver fibrosis (Fig. 2D). Compared with WT mice, *Cd73* KO mice presented elevated mRNA levels of proinflammatory cytokines (*Il17* and *Tnfa)* and fibrosis-related genes (*Col1a1*, *Col3a1,* and *Acta2*) after CDHFD feeding, but not hydroxyproline, suggesting that *Cd73* KO promoted MASLD progression in these mice (Figure 2E—G).

Next, we compared the lymphocyte composition in the liver between CDHFD-fed WT and *Cd73* KO mice. Compared with WT mice, *Cd73* deficiency increased the proportion of bone marrow-derived monocytes and promoted monocyte differentiation into proinflammatory subtypes, such as $Ly6C^{high}$, $Trem1^+$, and TNF-α^+ (Fig. S1K-S1M). We also found that the amount of IL-17A secreted by $CD4^+$ T cells was increased in *Cd73* KO mice (Fig. S1M). The above results suggest that CD73 altered the liver immune microenvironment in individuals with MASLD. Importantly, *Cd73* deficiency decreased the proportion (Figure 2H,I) of Tregs and suppressed Treg survival, as shown by increased Annexin V^+ and Caspase-3 activity and decreased Ki67 and BCL-2 expression (Fig. 2J). Furthermore, *Cd73* KO significantly inhibited the immunomodulatory activity of Tregs, resulting in decreased secretion of Granzyme B and IL-10 and decreased expression of CTLA4 and CD69, as shown in Fig. 2K-2N.

Next, we assessed the above results in MCD-fed mice to confirm the role of CD73 in MASLD. As expected, compared with WT mice, *Cd73* KO mice fed an MCD diet presented markedly increased plasma ALT, AST and TBIL levels and increased fat accumulation, lobular inflammation, and focal necrosis (Fig. S2A-S2C). The upregulated mRNA expression of *Col1a1*, *Col3a1*, and *Acta2,* indicating liver fibrosis, was exacerbated in the MCD-fed *Cd73* KO mice (Fig. S2D). Consistent with the findings in the CDHFD-fed MASLD model, *Cd73* deficiency increased the proportion of proinflammatory monocytes in MCD-fed mice, as well as Th1 and Th17 cells (Fig. S2E-S2H). Moreover, *Cd73* KO decreased the ratio of Tregs in $CD45^+$ immune cells or $CD4^+$ T cells and inhibited Treg survival and immunomodulation in MCD-fed mice (Fig. S2I-S2M). We also validated the effect of CD73 on immunomodulation by sorting Tregs from MCD-fed WT or *Cd73* KO mice and coculturing them with $CD3^+$ T cells *in vitro*. Compared with MCD diet-fed WT mice, *Cd73* KO mice presented reduced suppressive activity of Tregs (Fig. S2N). Taken together, these data revealed that *Cd73* deficiency significantly promoted MASLD progression and inhibited Treg survival and immunomodulation.

3.3. CD73 maintains Treg survival and immunomodulatory activity, protecting against MASLD progression

To further elucidate the role of CD73 in regulating Tregs in MASLD, we adoptively transferred WT mouse-derived $CD3^+$ T cells (W/WT Tregs) or $CD3^+$ T cells without Tregs (W/O Tregs) into $Rag1^{-/-}$ mice

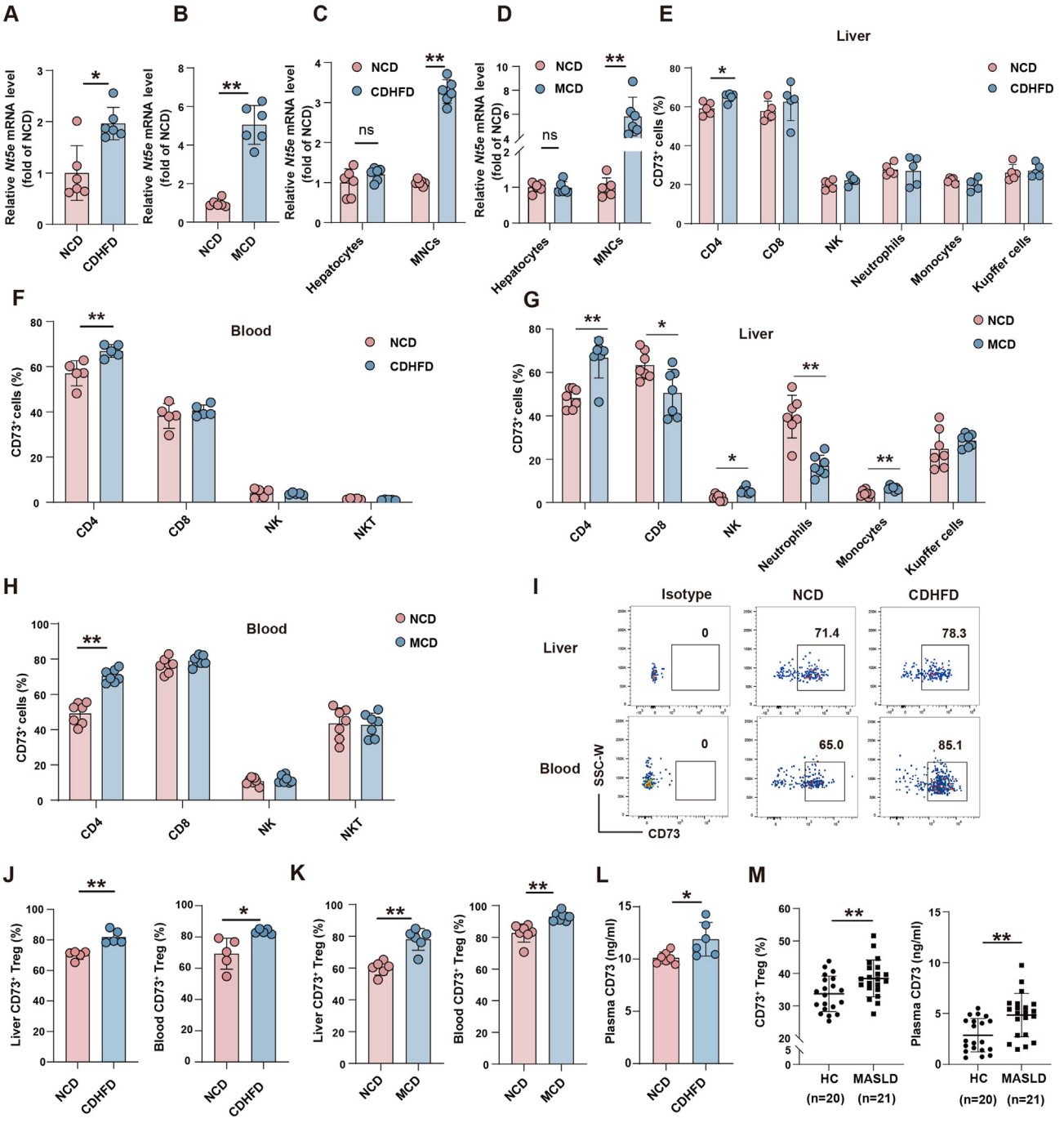

Figure 1: CD73 expression on Tregs is increased during MASLD progression.

(A—B). The mRNA levels of *Nt5e* in the livers of the MCD- or CDHFD-fed mice were determined by real-time PCR. (C—D). The *Nt5e* mRNA levels in hepatocytes or liver MNCs of the MCD- or CDHFD-fed mice were measured by real-time PCR. (E). CD73 expressions on liver $CD4^+$ T, $CD8^+$ T, NK cells, neutrophils, monocytes, and Kupffer cells were determined in NCD- and CDHFD-fed mice. (F). CD73 expressions on blood $CD4^+$ T, $CD8^+$ T, NK, and NKT cells were measured in NCD- and CDHFD-fed mice. (G). CD73 expressions on liver $CD4^+$ T, $CD8^+$ T, NK cells, neutrophils, monocytes, and Kupffer cells were determined in the NCD- and MCD-fed mice. (H). CD73 expressions on blood $CD4^+$ T, $CD8^+$ T, NK, and NKT cells were measured in the MCD-fed mice. (I). Representative flow cytometry plots of CD73 expression on Tregs ($CD4^+CD25^+CD127^-$) in the livers or blood of the CDHFD-fed mice. (J—K). Statistical analysis of the percentages of $CD73^+$ Tregs in the liver or blood of the CDHFD- and MCD-fed mice. (L). CD73 concentration in plasma was determined. (M). The ratio of $CD73^+$ Tregs in PBMCs (left) and the concentration of soluble CD73 in plasma (right) from the healthy controls or MASLD patients. n = 5—21 per group. $*P < 0.05$, $**P < 0.01$.

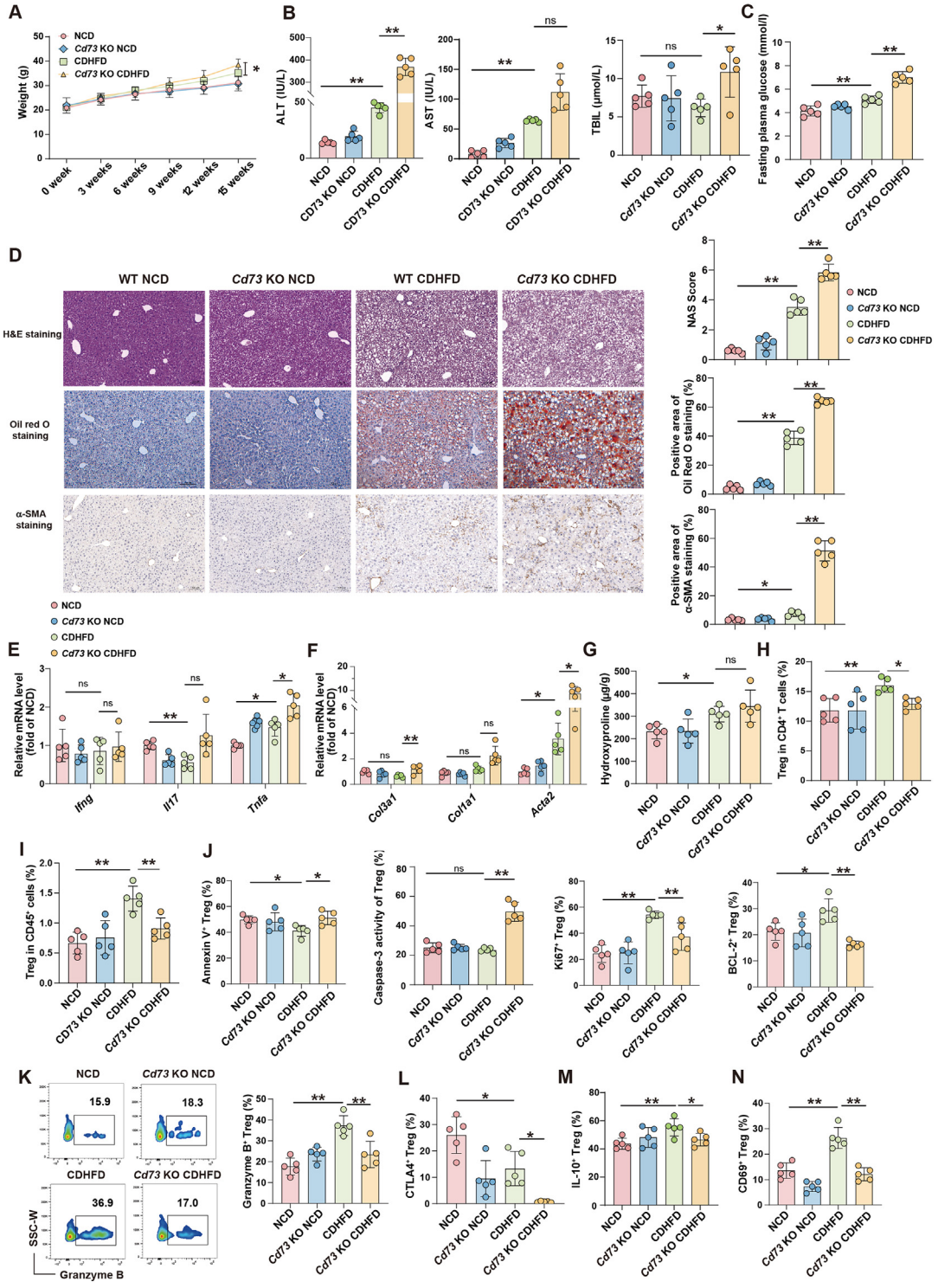

Figure 2: *Cd73* knockout decreases intrahepatic Treg survival and immunomodulatory activity in CDHFD-induced MASLD model.
(A). Body weight of the NCD- or CDHFD-fed WT or *Cd73* knockout mice. (B). Plasma ALT, AST, and TBIL levels were determined. (C). Fasting plasma glucose levels were determined in the NCD- or CDHFD-fed mice. (D). Representative H&E, Oil Red O, and α-SMA staining and quantification of liver histology staining. (E). The relative mRNA expressions of proinflammatory cytokines (*Ifng*, *Il17*, and *Tnfa*) in the liver were measured. (F). Fibrosis-related genes (*Col3a1*, *Col1a1*, and *Acta2*) were assessed by real-time PCR. (G). Hydroxyproline levels in liver tissues from the NCD- or CDHFD-fed mice. (H—I). Ratio of Tregs among liver $CD4^+$ T cells and $CD45^+$ cells. (J). Apoptosis (Annexin V, Caspase-3 activity) and proliferation (Ki67, BCL-2) of liver Tregs were detected by flow cytometry. (K). Representative flow cytometry plots and statistical analysis of Granzyme Bpositive Tregs in the liver. (L—N). Proportion of $CTLA4^+$, $IL\text{-}10^+$, and $CD69^+$ Tregs in each group of mice. n = 5 per group. $^*P < 0.05$, $^{**}P < 0.01$. (For interpretation of the references to color in this figure legend, the reader is referred to the Web version of this article.)

separately. Moreover, WT mouse-derived $CD3^+$ T cells without Tregs were mixed with *Cd73* KO mouse-derived Tregs and transferred into *Rag1*$^{-/-}$ mice (W/*Cd73* KO Tregs). Additionally, a control group of *Rag1*$^{-/-}$ mice that received no cell transfer was included. All the *Rag1*$^{-/-}$ mice were subsequently fed an MCD for 4 weeks (Figure 3A). Compared with those in control *Rag1*$^{-/-}$ mice, transferring $CD3^+$ T cells without Tregs markedly accelerated liver injury, as shown by increased plasma ALT and AST levels and severe liver inflammation and lipid accumulation, whereas supplementation with WT Tregs alleviated liver injury, but not *Cd73* KO Tregs (Figure 3B—E). In addition, considering that adoptively transferring $CD3^+$ T cells without Tregs into *Rag1*$^{-/-}$ mice might result in symptoms of colitis, we also monitored the body weights of the mice. As shown in Figure 3F, compared with control *Rag1*$^{-/-}$ mice, adoptively transferring $CD3^+$ T cells without Tregs significantly reduced body weight, whereas WT Tregs but not *Cd73* KO Tregs inhibited weight loss. We also measured the representative proinflammatory cytokines in plasma, e.g. TNF-α, IL-1β, IL-6, and IFN-γ. Compared with control *Rag1* KO mice, those in which $CD3^+$ T cells without Tregs were transferred presented increased levels of systemic inflammation. However, supplementation with WT Tregs but not *Cd73* KO Tregs decreased the levels of inflammatory cytokines (Fig. 3G). To determine whether the transferred Tregs in the adoptive transfer model could be recruited to the liver, we assessed their homing ability by detecting the frequencies of Tregs ($CD3^+CD4^+FOXP3^+$ subset) using flow cytometry. As expected, there was almost no Treg recruitment to the liver in the $CD3^+$ T cells without the Treg model, while a certain number of Tregs were detected in the livers of the W/WT Treg group, which was greater than that in the *Cd73* KO Treg group (Fig. 3H). In addition, *Cd73* deficiency in Tregs resulted in impaired cell viability and suppressive activity *in vivo* (Figure 3I,J). We also detected changes in the intrahepatic immune microenvironment. As shown in Fig. 3K-3M, the administration of $CD3^+$ T cells without Tregs exacerbated the proinflammatory response in the liver, whereas supplementation with WT Tregs significantly suppressed this inflammatory response, except *Cd73* KO Tregs. These results suggest that CD73 protects Tregs against MASLD by maintaining Treg viability and immunoregulatory activity.

3.4. FFAs increase CD73 expression on Tregs via the p38/Gata2 signaling pathway

To determine the mechanisms of CD73 upregulation on Tregs during MASLD progression, highly purified (>98% purity) Tregs ($CD4^+CD25^+CD127^-$ T cells) isolated from the livers of MCD- or NCD-fed WT mice were compared via transcriptome sequencing (Fig. S3A). GSEA, KEGG and Gene Ontology (GO) pathway analyses revealed that MCD promoted fatty acid metabolic processes, including cholesterol metabolism and fat digestion and absorption (Figure 4A and S3B—S3C). Therefore, we hypothesized that a lipid-accumulating environment in MASLD has the potential to increase CD73 expression on Tregs. To test this hypothesis, we stimulated Tregs with FFAs (a mixture of oleic acid and palmitic acid at a ratio of 2:1) for 48 h, and CD73 expression was significantly upregulated (Fig. 4B). KEGG and GO pathway analyses also revealed that MASLD promoted the MAPK and PI3K-AKT signaling pathways in Tregs (Fig. S3B). In an *in vitro* study involving FFAs stimulation, we confirmed that FFAs increased the levels of phosphorylated AKT and MAPK signaling pathway components (including phosphorylated ERK1/2 and p38) but decreased the level of phosphorylated JNK (Figure 4C,D). The p38 inhibitor (SB203580), but not the AKT inhibitor (MK2206) or ERK1/2 inhibitor (PD98059), reversed the effect of FFAs on Tregs, suggesting that p38 signaling contributes to the upregulation of CD73 expression on Tregs (Fig. 4E). To further explore how p38 transduces intranuclear signals and promotes *Nt5e* (encoding CD73) transcription in Tregs, we predicted the transcription factor-binding sites of the *Nt5e* promoter region via the JASPAR CORE database. Four transcription factors (*Runx2*, *Gata2*, *Sox9*, and *Tcf4*) were found at the intersection of transcription factor-binding sites and DEGs in Tregs from MCD- versus NCD-fed mice (Fig. 4F). Among the four transcription factors, only *Gata2* was elevated after FFAs treatment and downregulated after treatment with a p38 inhibitor (SB203580), suggesting that the p38/Gata2 signaling pathway plays a key role (Figure 4G—I). A CUT&Tag assay was subsequently performed to explore the Gata2 binding sites, and the peak distribution was found near the *Nt5e* promoter region (Fig. 4J). Real-time PCR confirmed that FFAs treatment significantly increased *Gata2* binding at the *Nt5e* promoter site (Fig. 4K). Further study revealed that the GATA2 inhibitor K7174 successfully abolished the FFAs induced increase in CD73 expression in Tregs (Fig. 4L), indicating that FFAs upregulate CD73 expression via the p38/Gata2 signaling pathway.

3.5. CD73 protects Tregs from AMP-induced toxicity, while the degradation product adenosine promotes Treg survival and function in the presence of FFAs

Transcriptome sequencing was also performed to compare Tregs from MCD-fed WT and *Cd73* KO mice. Consistent with the flow cytometry results, *Cd73* knockout decreased leukocyte-mediated cytotoxicity and increased apoptosis in Tregs from the MASLD group (Fig. S3D-S3H). In addition, we analyzed 24-week scRNA-seq data from the GSE156059 dataset to confirm the effect of CD73 on liver Tregs within a WD-induced MASLD mouse model. This data exhibited temporal consistency with our established WD feeding protocol and better simulated diet-induced metabolic imbalance, while the limited sample size (one biological replicate) might constitute a notable statistical limitation. As shown in Fig. S4A and S4B, Tregs were identified based on the coexpression of *Cd3d, Cd3e, Cd3g, Cd4*, and *Foxp3*. The expression of *Nt5e* (*Cd73*) in the WD model was significantly greater than that in the control group (Fig. S4C). Compared with *Cd73*$^-$ Tregs, *Cd73*$^+$ Tregs from WD-fed mice highly expressed the functional molecules *Il10, Tgfb1, Lag3* and downregulated *Havcr2* (Tim-3), and highly upregulated the transcription factor *Gata2*, which could promote CD73 expression on Tregs (Fig. S4D). And *Cd73*$^+$ Tregs also increased the expression of the antiapoptotic gene *Bcl2l12* and downregulated *Tnfrsf10b* (DR5). In addition, enrichment pathway analysis revealed that CD73 enhanced Treg homeostasis, fatty acid metabolic process, and cell viability, findings similar to those of CDHFD- or MCD-fed mouse models (Fig. S4E). Therefore, we further explored the mechanisms by which *Cd73* knockout affects Treg survival and function in MASLD.

CD73 is a key ecto-5′-nucleotidase that catalyzes AMP, which is derived from ATP degradation by CD39 and produces adenosine (ADO). Hence, we investigated whether CD73 is an ectonucleotidase that regulates Treg functions in MASLD. Compared with WT mice, *Cd73* deficiency did not change the plasma ATP content but significantly elevated AMP and decreased the ADO concentration in CDHFD- and MCD-fed mice and in MCD-fed mice with *Cd73*-specific knockout in Tregs (Figure 5A—C). An *in vitro* assay with additional ATP stimulation also revealed the critical role of CD73 in the conversion of AMP to ADO in Tregs (Fig. 5D), suggesting that distinct variations in plasma AMP and ADO levels *in vivo* might result from CD73 expression on Tregs. Combined with previous results showing that *Cd73* KO affects Treg apoptosis and function *in vivo*, we hypothesize that an imbalance in AMP/ADO influences Treg viability and the immune microenvironment.

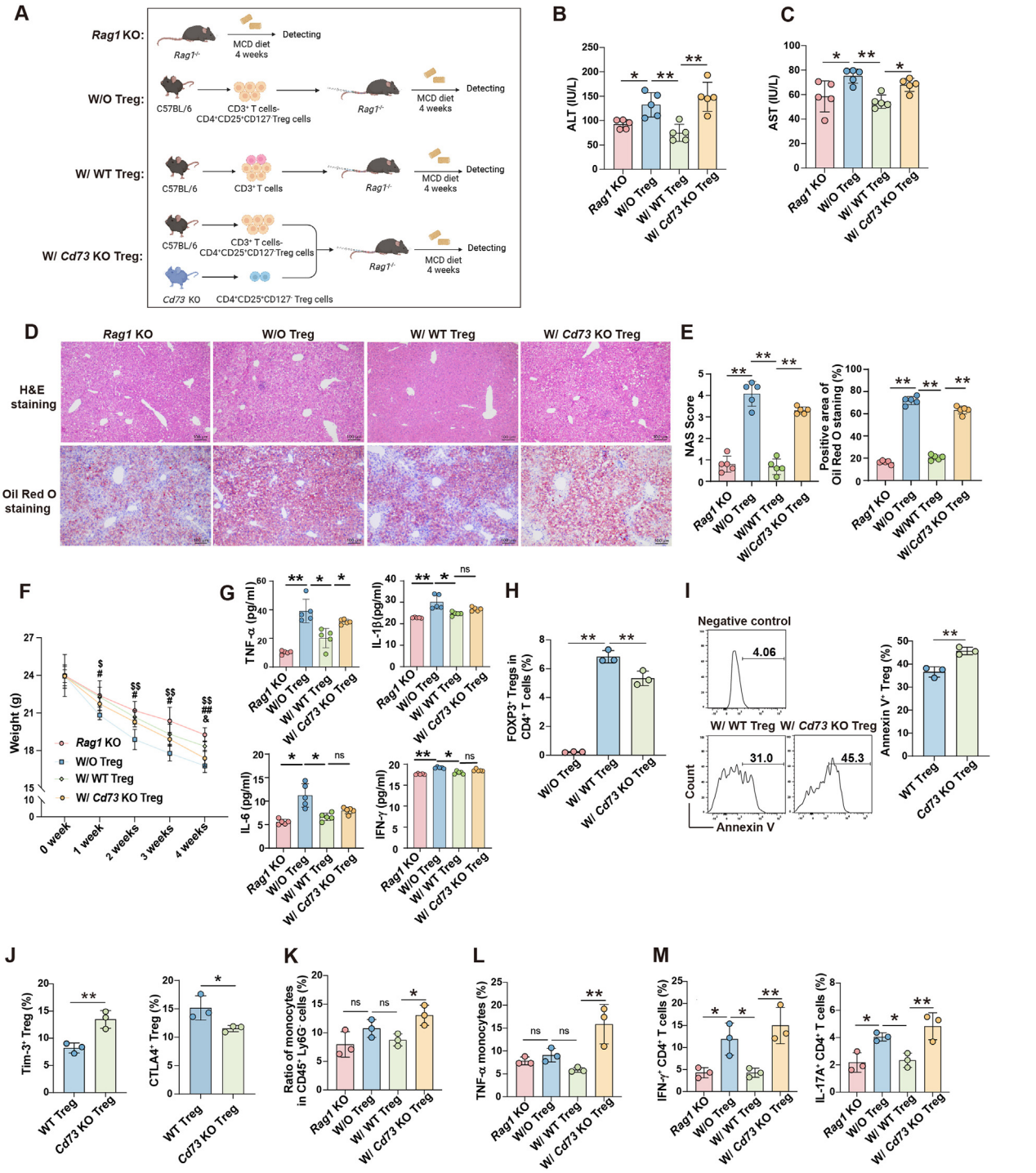

Figure 3: CD73 maintains Treg survival and immunomodulatory activity, protecting against MASLD progression.
(A). The *Rag1*$^{-/-}$ mice were adoptively transferred with WT mouse-derived CD3^{+} T cells (W/WT Treg group) or CD3^{+} T cells without Tregs (W/O Treg group). In the W/*Cd73* KO Treg group, *Rag1*$^{-/-}$ mice received CD3^{+} T cells without Tregs (from WT mice) together with *Cd73* KO Tregs (from *Cd73* KO mice). The above recipient mice and control *Rag1*$^{-/-}$ mice not receiving cell transfer were subsequently fed MCD for 4 weeks. Created in https://BioRender.com. (B—C). Plasma ALT and AST levels were determined. (D). H&E and Oil Red O staining of representative paraffin-embedded liver sections. (E). Quantification of liver H&E and Oil Red O staining. (F). The body weight of mice at a different time. (G). The cytokine levels in plasma were measured by ELISA. (H) Ratio of CD4^{+}FOXP3^{+} Tregs in liver CD4^{+} T cells. (I, J) Ratio of Annexin V^{+}, Tim-3^{+}, CTLA4^{+} Tregs in the livers of transplanted *Rag1*$^{-/-}$ mice. (K). Ratio of monocytes (CD11b^{high}F4/80^{low}) in liver CD45^{+}Ly6G^{-} cells. (L). The level of TNF-α secreted by monocytes was detected. (M). Ratio of Th1 (IFN-γ^{+}) or Th17 (IL-17^{+}) in CD4^{+} T cells. n = 3—5 per group. *$P < 0.05$, **$P < 0.01$. $: A comparison between group *Rag1* KO and W/O Treg with $P < 0.05$; $$: A comparison between group *Rag1* KO and W/O Treg with $P < 0.01$; #: A comparison between group W/O Treg and W/WT Treg with $P < 0.05$; ##: A comparison between group W/O Treg and W/WT Treg with $P < 0.01$; &: A comparison between group W/WT Treg and W/*Cd73* KO Treg with $P < 0.05$. (For interpretation of the references to color in this figure legend, the reader is referred to the Web version of this article.)

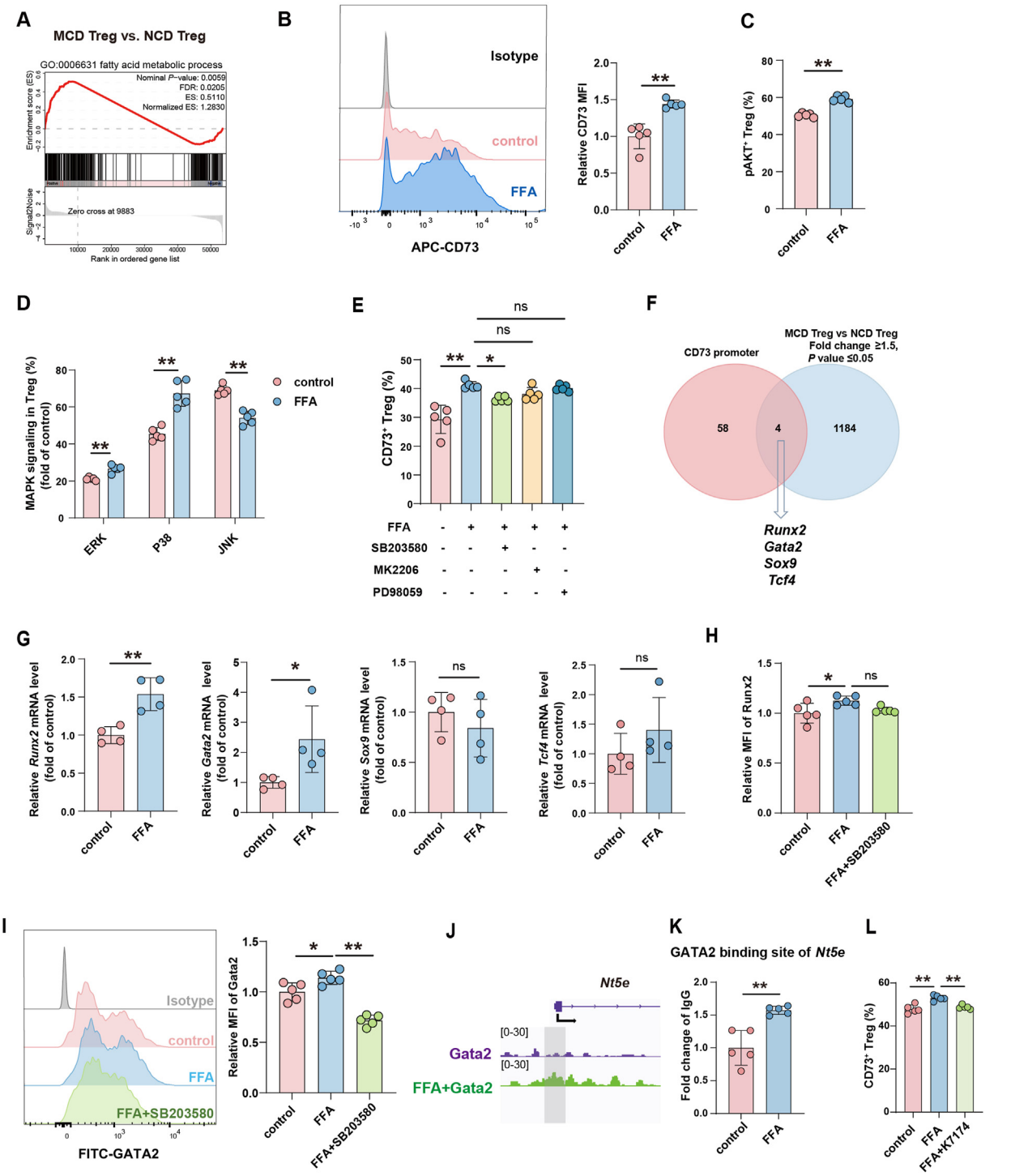

Figure 4: FFAs increase CD73 expression on Tregs via p38/Gata2 signaling pathway.
(A). GSEA of Tregs from MCD-versus NCD-fed mice was performed. (B) After the addition of FFAs for 48 h, the expression of CD73 on Tregs was measured by flow cytometry. (C) Phosphorylated AKT activity in the Tregs after FFAs treatment. (D). MAPK signaling was detected in FFAs-stimulated Tregs by flow cytometry. (E). Tregs isolated from WT mice were preincubated with p38 inhibitor (SB203580), AKT inhibitor (MK2206), or ERK1/2 inhibitor (PD98059) for 1 h followed by FFAs treatment for 48 h, and the CD73 expression was detected by flow cytometry. (F). Transcription factor-binding sites of the *Nt5e* promoter region were predicted through the JASPAR CORE database and intersected with DEGs of Tregs from MCD- versus NCD-fed mice. (G). Relative mRNA levels of transcription factors (*Runx2, Gata2, Sox9*, and *Tcf4*) were determined by real-time PCR. (H—I). Runx2 and Gata2 expression was detected in Tregs incubated with p38 inhibitor (SB203580) followed by FFAs stimulation. (J). CUT&Tag assays of GATA2 binding sites showed a peak distribution around the *Nt5e* promoter region in the FFAs-treated Tregs. (K). The enrichment of GATA2 binding sites in the *Nt5e* promoter region was confirmed by real-time PCR, and the data were normalized to those of IgG. (L). CD73 expression on Tregs with pre-treatment of Gata2 inhibitor (K7174) and subsequent FFA stimulation. n = 4—5 per group. $^{*}P < 0.05$, $^{**}P < 0.01$.

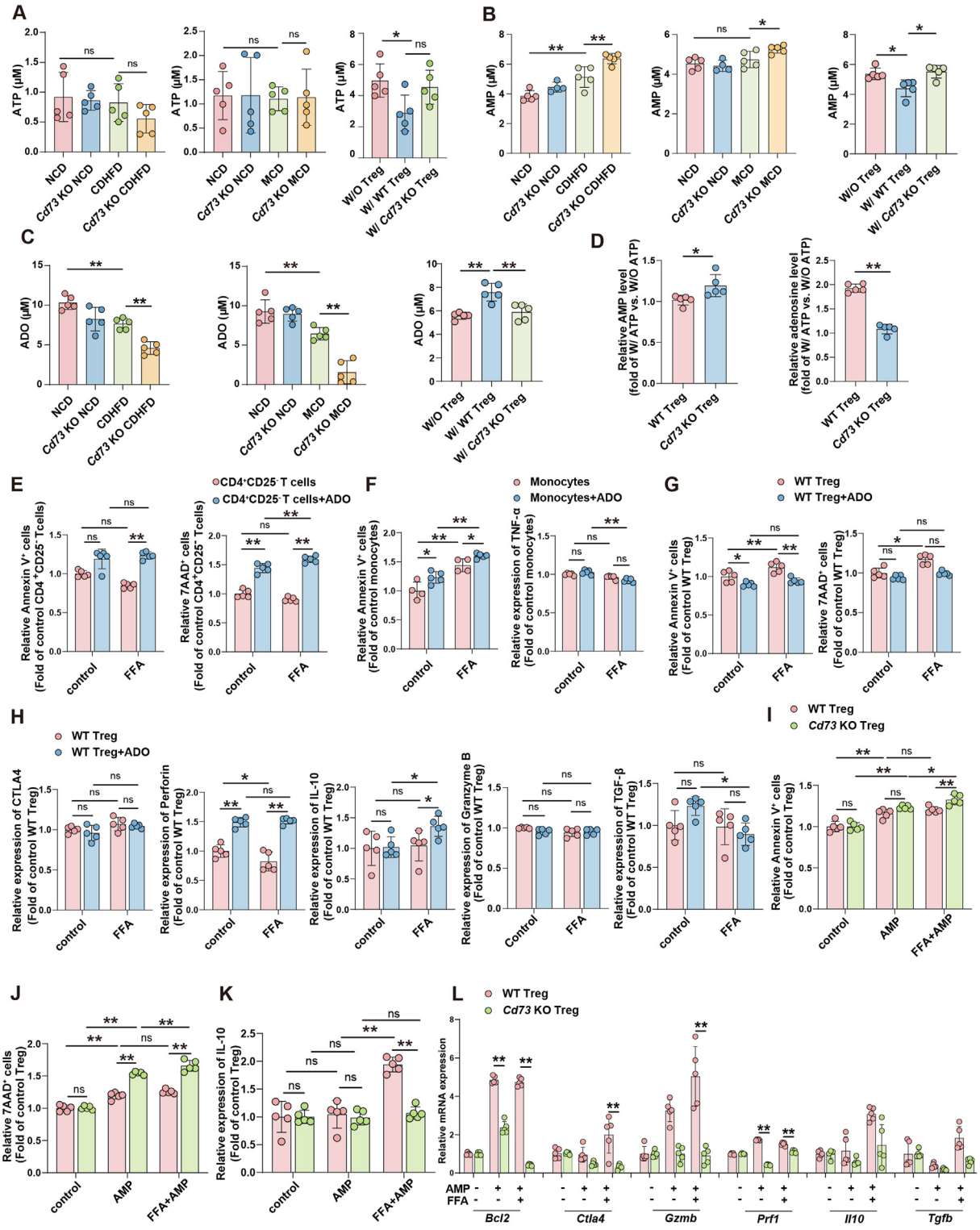

Figure 5: CD73 protects Tregs from AMP-induced toxicity, while the degradation product adenosine promotes Treg survival and function in the presence of FFAs. (A—C). The plasma concentrations of ATP, AMP, and adenosine (ADO) were measured in the CDHFD- or MCD-fed WT and *Cd73* KO mice, as well as the MCD-fed Treg-transplanted *Rag1*$^{-/-}$ mice. (D) Relative AMP and ADO levels in the supernatant after the addition of ATP to cultures of WT or *Cd73* KO Tregs. (E). Apoptosis of CD4^{+} T cells without Tregs was detected after ADO treatment with or without FFAs treatment. (F). Apoptosis and TNF-α secretion were measured in ADO-stimulated monocytes with or without FFAs treatment. (G). Apoptosis of ADO-stimulated Tregs was detected by flow cytometry. (H). The expression of immunomodulatory molecules (CTLA4, Perforin, IL-10, Granzyme B, and TGF-β) on WT Tregs were detected after ADO stimulation with or without FFAs treatment. (I—K). Treg apoptosis (Annexin V and 7AAD) and IL-10 expression were compared between WT and *Cd73* KO mice after AMP supplement with or without FFAs treatment. (L) The relative mRNA expression of *Bcl2, Ctla4, Gzmb, Prf1, Il10*, and *Tgfb* in Tregs from WT and *Cd73* KO mice was determined after AMP supplement with or without FFAs treatment. n = 4—5 per group. $^{*}P < 0.05$, $^{**}P < 0.01$.

To confirm the effects of adenosine on immune cells, such as monocytes, $CD4^+$ T cells, and Tregs, which are important effector cells in MASLD, we treated monocytes with or without LPS or sorted naïve Tregs and $CD4^+$ $CD25^-$ cells ($CD4^+$ T cells without Tregs) with or without anti-CD3/CD28 beads and then observed changes in the mRNA expression of adenosine receptors. All adenosine receptor levels increased to different degrees in monocytes, $CD4^+CD25^-$ T cells, and Tregs after stimulation (Fig. S3I and S3J), indicating that adenosine might affect immune cell activation. Interestingly, under basal control or FFAs induced conditions, we found that ADO treatment markedly inhibited the survival and activation of proinflammatory effector cells ($CD4^+$ $CD25^-$ T cells and monocytes, Figure 5E,F), but increased Treg viability and activation (Figure 5G—H), suggesting that ADO acts as an immunoregulatory factor and has different effects on proinflammatory and immunoregulatory cells.

Moreover, the viability of Tregs did not significantly differ between WT and *Cd73* KO mice under normal conditions. However, AMP stimulation decreased WT Treg viability, whereas *Cd73* deficiency significantly increased this effect, especially with FFAs supplementation (Fig. 5I-5L). Taken together, these data show that CD73 is an important hydrolytic enzyme that converts the toxicant AMP into the immunoregulatory factor ADO, which is critical for maintaining Treg viability and function during MASLD progression.

3.6. CD73 inhibits Treg apoptosis by suppressing the TRAIL-DR5 interaction

Deletion of *Cd73* in mice with MASLD significantly increased Treg apoptosis (Fig. S3E and S3G), however, the factors affecting Treg survival and apoptosis remain unclear. TRAIL-DR5 (TRAIL-RII) is one of the most common signaling pathways closely related to cell death. We found that the liver expression levels of *Tnfrsf10b* (DR5) and *Tnfsf10* (TRAIL) were increased in CDHFD- and MCD-fed WT mice, suggesting that MASLD activated the TRAIL-DR5 signaling pathway (Figs. 6A and S3K). Moreover, the CDHFD-fed mice presented increased levels of TRAIL (Figure 6B), and the proportions of $DR5^+$ Tregs were increased in the MASLD model (Fig. 6C).

To study the effect of CD73 on TRAIL-DR5 signaling, we added FFAs and TRAIL proteins to Tregs or $CD4^+$ effector cells ($CD4^+CD25^-$) for 48 h. TRAIL significantly increased the apoptosis of $CD4^+$ effector T cells but not that of Tregs under FFAs stimulation (Fig. 6D). We speculated that this finding might be related to the high expression of CD73 on Tregs, which could interfere with the combination of TRAIL and DR5. To confirm our speculation, we divided Tregs into three groups ($CD73^{high}$, $CD73^{int}$ and $CD73^{neg}$) according to the level of CD73 expression and found that the greater the expression of CD73 was, the lower the level of apoptosis induced by FFAs and TRAIL (Fig. 6E), suggesting that TRAIL-induced cell apoptosis was inhibited by highly expressed CD73 on Tregs. Tregs from WT or *Cd73* KO mice were treated with FFAs and TRAIL to further validate the role of CD73 in the TRAIL-DR5-mediated cell death signaling pathway. Compared with WT Tregs, TRAIL noticeably promoted *Cd73* KO Treg apoptosis (Figure 6F,G). Finally, we pretreated Tregs with the CD73 protein to block DR5 in Tregs and then treated the Tregs with the TRAIL protein. The results showed that the CD73 protein successfully rescued Tregs from apoptosis, suggesting that CD73 increased Treg survival by suppressing the TRAIL-DR5 interaction under fatty acid conditions (Fig. 6H).

4. DISCUSSION

Tregs act as key regulators of immune regulation by limiting the inflammatory response and maintaining immune homeostasis. Previous studies have shown that an imbalance in the Th17/Treg ratio promotes the pathogenesis of MASLD in mice and humans [25], however the specific mechanism of Tregs in MASLD needs to be further studied. Here, we note that CD73 is a key molecule that regulates the role of Tregs in MASLD by inhibiting the liver proinflammatory environment and promoting Treg viability and activity. Specifically, CD73 modulated Treg function via enzymatic- and nonenzymatic-mediated pathways (Fig. 6I).

In this study, we established a MASLD mouse model by feeding a CDHFD or MCD and found that CD73 expression on Tregs was significantly increased in mice with MASLD. Similar alterations in CD73 expression on Tregs were also observed in the PBMCs of MASLD patients and were strongly correlated with MASLD pathogenesis. This phenomenon is related to previous reports showing increased in CD73 expression under inflammatory conditions [26]. In addition to the cell membrane-bound form of CD73, a soluble variant of the CD73 protein has also been detected in human plasma and serum, and a CD73 inhibitor blocked this AMPase activity, confirming the presence of soluble CD73 [27]. We detected an increase in soluble CD73 in the plasma of both MASLD mice and MASLD patients. Further transcriptome sequencing studies suggested that alterations in CD73 expression might be related to the unique liver environment in MASLD, which is characterized by FFAs accumulation. Previous reports have shown that unsaturated fatty acids increase the expression and enzyme activity of CD73 on endothelial cells [28,29]. Our study revealed that FFAs upregulated CD73 expression on Tregs via the p38 signaling pathway-mediated transcription factor GATA2. GATA2, a critical regulator of hematopoiesis, and mutation of *GATA2* results in monocytopenia, deficiencies in dendritic and B cells, and eventhe absence of Tregs [30]. Here, we found that GATA2 was the key molecule that upregulated CD73 expression on Tregs, increasing Treg viability and immunoregulatory activity.

Previous studies on ectonucleotidases in Tregs have focused on CD39 rather than CD73, as CD39 is an important effector molecule in Tregs that suppresses immunity and controls autoimmune diseases [31—33]. CD73 has also been reported to play a critical role in concert with CD39 in generating adenosine to increase Treg suppressive activity [34]. This study investigated whether CD73 could modulate Tregs to limit the intrahepatic inflammatory response. Adoptively transferring CD73-expressing Tregs into $Rag1^{-/-}$ mice revealed that Treg-mediated protection was effective, while CD73 deficiency significantly impacted Treg survival and activity and exacerbated MASLD progression, suggesting that CD73 plays a critical role in Treg-mediated immunosuppression. In addition, except for MCD-induced MASLD, adoptive transfer of $CD3^+$ T cells without Tregs into $Rag1^{-/-}$ mice also induced a systemic response, accompanied by abnormal changes in body weight and inflammatory cytokine levels in plasma. These findings suggest that the weight loss and secretion of inflammatory cytokines in this mouse model may result from both colitis and the MCD diet. To investigate the role of CD73 in regulating Treg function during MASLD progression, we focused primarily on evaluating liver steatosis and inflammatory response. Our data revealed that Tregs influence both the progression of MASLD and systemic conditions, such as colitis, in a CD73-dependent manner.

CD73 is a key ectonucleotidase that catabolizes AMP into the subsequent purine metabolite adenosine. Similarly, we discovered that *Cd73* KO markedly elevated AMP and decreased ADO levels both in the plasma of mice with MASLD and *in vitro* in Tregs stimulated with ATP. Intracellular AMP is an important metabolite that regulates cell growth and energy metabolism by activating the AMPK signaling pathway [35]. However, the released extracellular AMP is rapidly hydrolyzed into

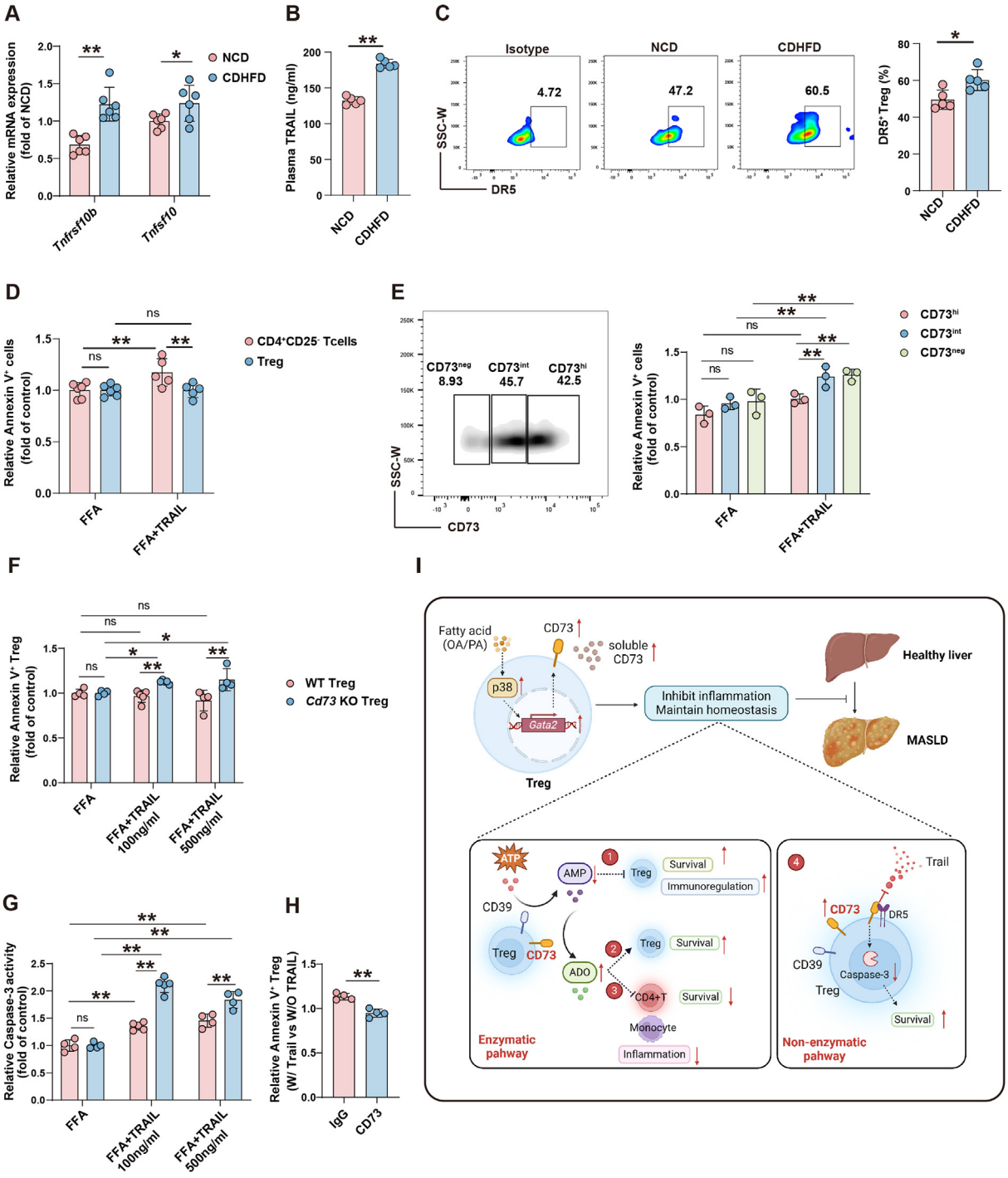

Figure 6: CD73 inhibits Treg apoptosis by suppressing the TRAIL-DR5 interaction.
(A). The relative mRNA expression of *Tnfrsf10b* (DR5) and *Tnfsf10* (TRAIL) in the liver was measured by real-time PCR. (B). Plasma content of TRAIL in the CDHFD- or NCD-fed mice. (C). DR5 expression on liver Tregs. (D). Relative apoptotic levels were compared between $CD4^+$ T cells without Tregs and Tregs followed by FFAs treatment with or without TRAIL. (E). Relative apoptotic levels were compared among $CD73^{high}$, $CD73^{int}$ and $CD73^{neg}$ Tregs after FFAs treatment with or without TRAIL. (F–G). Relative Annexin V and Caspase-3 activity were measured in the WT and *Cd73* KO Tregs treated with FFAs with or without TRAIL. (H). Tregs were blocked with CD73 protein or IgG for 6 h, followed by the addition of FFAs and TRAIL for 48 h. The proportions of Annexin V^+ Tregs after TRAIL supplement. (I). CD73 on Tregs limits inflammation and maintains homeostasis during MASLD progression (Created in https://BioRender.com). n = 3–6 per group. $^*P < 0.05$, $^{**}P < 0.01$.

adenosine, suppressing proinflammatory mediators' secretion by neutrophils and macrophages [36,37]. Therefore, the inherent role of extracellular AMP in immune cell growth and function is still unclear. Excessive extracellular AMP was an important factor limiting Treg survival, especially with FFAs supplementation. Our data revealed that depletion of CD73 in Tregs induced an imbalance in AMP/adenosine, and high levels of AMP could directly mediate Treg apoptosis and inactivation, suggesting that CD73 plays a critical role as an ectonucleotidase. In combination with other nucleotides, adenosine is critical in inflammatory effects. In T cells, adenosine reduces IL-2 generation to suppress effector T-cell proliferation, whereas A2A adenosine receptor engagement increases the expression of Foxp3 to restore Treg function [38,39]. The expression of CD39 and CD73, and their catabolic ability to secrete adenosine are also related to M1/M2 differentiation and cytokine production in monocytes [40]. Similarly, this study found that adenosine generated by Tregs limited the survival and activation of $CD4^+$ T cells and monocytes while increasing Treg activity and viability.

Transcriptome sequencing analysis revealed that CD73 deficiency hampered Treg immunomodulatory function and limited cell viability. We also acknowledge that the relatively small sample size ($n = 2-3$ per group) in our RNA-seq analysis has statistical limitation, future studies with larger sample sizes will address this issue. A previous report showed that CD73 blocks TRAIL-DR5 activity in Jurkat cells, thereby inhibiting cell apoptosis [41]. We found that TRAIL-DR5 signaling was strongly activated in MASLD-affected livers. TRAIL together with fatty acids in the liver environment of MASLD syndrome patients caused Treg apoptosis, and this unique environment also increased the expression of CD73 on Tregs, which were able to resist TRAIL-induced cell death by blocking the TRAIL-DR5 interaction.

Several limitations in this study need to be addressed. CD73 is an ectonucleotidase expressed on various types of cells. Snider et al. have reported that hepatocyte specific *Nt5e* (CD73) knockout could lead to MASLD phenotypes in middle-aged male mice, suggesting the important effect of hepatocyte CD73 on liver metabolic homeostasis under physiological conditions [42]. In the MASLD mouse model, we found that global knockout of *Cd73* significantly enhanced the proinflammatory effects on T cells and monocytes. Therefore, we cannot rule out the possibility that CD73 directly affects other immune cells or that CD73 regulates Tregs during MASLD progression. Moreover, we used both global *Cd73* knockout mice and specifically adoptively transferred *Cd73* knockout Tregs to identify the effect of CD73 on Tregs during MASLD, while the exact role of CD73 on Tregs in a more physiologically relevant manner in Treg-specific *Cd73* knockout mice will be dissected.

In summary, CD73 increases Treg survival and immunomodulatory functions to inhibit MASLD progression. FFAs increased CD73 expression on Tregs via p38/GATA2 signaling during MASLD progression. CD73 promoted Treg survival and function via enzymatic and nonenzymatic pathways, limiting the inflammatory response and maintaining liver immune homeostasis (Fig. 6I). Our study not only reveals the mechanism by which Tregs inhibit intrahepatic inflammation but also provides important immunological markers for the diagnosis of the degree of intrahepatic inflammation in MASLD patients.

CRediT AUTHORSHIP CONTRIBUTION STATEMENT

Hua Jin: Writing — original draft, Methodology, Investigation, Funding acquisition, Formal analysis, Data curation. **Xinjie Zhong:** Writing — original draft, Methodology, Investigation, Formal analysis, Data curation. **Chunpan Zhang:** Investigation, Validation, Methodology, Formal analysis. **Yongle Wu:** Resources. **Jie Sun:** Software, Methodology. **Xiyu Wang:** Software, Methodology. **Zeyu Wang:** Methodology, Formal analysis. **Jingjing Zhu:** Methodology, Formal analysis. **Yuan Jiang:** Methodology, Formal analysis. **Xiaonan Du:** Methodology, Formal analysis. **Zihan Zhang:** Methodology, Formal analysis. **Dong Zhang:** Writing — review & editing, Funding acquisition. **Guangyong Sun:** Writing — review & editing, Supervision, Project administration, Validation, Funding acquisition.

DECLARATION OF COMPETING INTEREST

All authors declare no conflicts of interest.

FINANCIAL SUPPORT STATEMENT

Grants from the National Natural Science Foundation of China (No. 82370578, 82300596, 82202021 and 82270606), the Beijing Natural Science Foundation (7232034), R&D Program of Beijing Municipal Education Commission (No. KZ202210025036), Beijing Municipal Administration of Hospitals' Ascent Plan (No. DFL20220103), Chinese Institutes for Medical Research, Beijing (No. CX24PY16) and the Youth Beijing Scholar (No. 035) supported this work.

DATA AVAILABILITY

Data will be made available on request.

APPENDIX A. SUPPLEMENTARY DATA

Supplementary data to this article can be found online at https://doi.org/10.1016/j.molmet.2025.102131.

LIST OF ABBREVIATIONS

ADO
adenosine
ALT
alanine aminotransferase
AMP
adenosine monophosphate
α-SMA
α-smooth muscle actin
AST
aspartate aminotransferase
ATP
adenosine triphosphate
CDE
choline-deficient and ethionine-supplemented
CDHFD
choline-deficient high-fat diet
DEGs
differentially expressed genes
FFAs
free fatty acids
GO
Gene Ontology
GSEA
gene set enrichment analysis
H&E
hematoxylin and eosin
HCC

hepatocellular carcinoma
KEGG
Kyoto Encyclopedia of Genes and Genomes
KO
knockout
MCD
methionine/choline-deficient diet
MNCs
mononuclear cells
MASLD
metabolic dysfunction-associated steatotic liver disease
MASH
metabolic dysfunction-associated steatohepatitis
NCD
normal control diet
PBMCs
peripheral blood mononuclear cells
Treg
regulatory T cells
WD
western diet
WT
wild-type

REFERENCES

[1] Younossi Z, Anstee QM, Marietti M, Hardy T, Henry L, Eslam M, et al. Global burden of NAFLD and NASH: trends, predictions, risk factors and prevention. Nat Rev Gastroenterol Hepatol 2018;15(1):11–20.

[2] Arab JP, Arrese M, Trauner M. Recent insights into the pathogenesis of nonalcoholic fatty liver disease. Annu Rev Pathol 2018;13(1):321–50.

[3] Younossi ZM. Non-alcoholic fatty liver disease – a global public health perspective. J Hepatol 2019;70(3):531–44.

[4] Simon TG, Roelstraete B, Khalili H, Hagström H, Ludvigsson JF. Mortality in biopsy-confirmed nonalcoholic fatty liver disease: results from a nationwide cohort. Gut 2021;70(7):1375–82.

[5] Eslam M, Sanyal AJ, George J, Sanyal A, Neuschwander-Tetri B, Tiribelli C, et al. MAFLD: a consensus-driven proposed nomenclature for metabolic associated fatty liver disease. Gastroenterology 2020;158(7):1999–2014.e1991.

[6] Yahoo N, Dudek M, Knolle P, Heikenwälder M. Role of immune responses in the development of NAFLD-associated liver cancer and prospects for therapeutic modulation. J Hepatol 2023;79(2):538–51.

[7] Tilg H, Adolph TE, Dudek M, Knolle P. Non-alcoholic fatty liver disease: the interplay between metabolism, microbes and immunity. Nat Metab 2021;3(12):1596–607.

[8] Huby T, Gautier EL. Immune cell-mediated features of non-alcoholic steatohepatitis. Nat Rev Immunol 2022;22(7):429–43.

[9] Wu K-J, Qian Q-F, Zhou J-R, Sun D-L, Duan Y-F, Zhu X, et al. Regulatory T cells (Tregs) in liver fibrosis. Cell Death Discovery 2023;9(1).

[10] Van Herck MA, Weyler J, Kwanten WJ, Dirinck EL, De Winter BY, Francque SM, et al. The differential roles of T cells in non-alcoholic fatty liver disease and obesity. Front Immunol 2019;10.

[11] Vignali DAA, Collison LW, Workman CJ. How regulatory T cells work. Nat Rev Immunol 2008;8(7):523–32.

[12] Riaz F, Wei P, Pan F. Fine-tuning of regulatory T cells is indispensable for the metabolic steatosis-related hepatocellular carcinoma: a review. Front Cell Dev Biol 2022;10.

[13] Ma X, Hua J, Mohamood AR, Hamad ARA, Ravi R, Li Z. A high-fat diet and regulatory T cells influence susceptibility to endotoxin-induced liver injury. Hepatology 2007;46(5):1519–29.

[14] Deaglio S, Dwyer KM, Gao W, Friedman D, Usheva A, Erat A, et al. Adenosine generation catalyzed by CD39 and CD73 expressed on regulatory T cells mediates immune suppression. J Exp Med 2007;204(6):1257–65.

[15] Alcedo KP, Bowser JL, Snider NT. The elegant complexity of mammalian ecto-5′-nucleotidase (CD73). Trends Cell Biol 2021;31(10):829–42.

[16] Li Y, Lu Y, Lin S-H, Li N, Han Y, Huang Q, et al. Insulin signaling establishes a developmental trajectory of adipose regulatory T cells. Nat Immunol 2021;22(9):1175–85.

[17] Müller G, Schneider M, Biemer-Daub G, Wied S. Upregulation of lipid synthesis in small rat adipocytes by microvesicle-associated CD73 from large adipocytes. Obesity 2011;19(8):1531–44.

[18] Shi W, Wang Y, Zhang C, Jin H, Zeng Z, Wei L, et al. Isolation and purification of immune cells from the liver. Int Immunopharmacol 2020;85.

[19] Guo R, Zhao B, Wang Y, Wu D, Wang Y, Yu Y, et al. Cichoric acid prevents free-fatty-acid-induced lipid metabolism disorders via regulating Bmal1 in HepG2 cells. J Agric Food Chem 2018;66(37):9667–78.

[20] Rinella ME, Lazarus JV, Ratziu V, Francque SM, Sanyal AJ, Kanwal F, et al. A multisociety Delphi consensus statement on new fatty liver disease nomenclature. J Hepatol 2023;79(6):1542–56.

[21] Carbone F, De Rosa V, Carrieri PB, Montella S, Bruzzese D, Porcellini A, et al. Regulatory T cell proliferative potential is impaired in human autoimmune disease. Nat Med 2014;20(1):69–74.

[22] Narula M, Lakshmanan U, Borna S, Schulze JJ, Holmes TH, Harre N, et al. Epigenetic and immunological indicators of IPEX disease in subjects with FOXP3 gene mutation. J Allergy Clin Immunol 2023;151(1):233–246 e210.

[23] Liu W, Putnam AL, Xu-Yu Z, Szot GL, Lee MR, Zhu S, et al. CD127 expression inversely correlates with FoxP3 and suppressive function of human CD4+ T reg cells. J Exp Med 2006;203(7):1701–11.

[24] Baecher-Allan C, Brown JA, Freeman GJ, Hafler DA. CD4+CD25high regulatory cells in human peripheral blood. J Immunol 2001;167(3):1245–53.

[25] He B, Wu L, Xie W, Shao Y, Jiang J, Zhao Z, et al. The imbalance of Th17/Treg cells is involved in the progression of nonalcoholic fatty liver disease in mice. BMC Immunol 2017;18(1).

[26] Doherty GA, Bai A, Hanidziar D, Longhi MS, Lawlor GO, Putheti P, et al. CD 73 is a phenotypic marker of effector memory Th17 cells in inflammatory bowel disease. Eur J Immunol 2012;42(11):3062–72.

[27] Schneider E, Rissiek A, Winzer R, Puig B, Rissiek B, Haag F, et al. Generation and function of non-cell-bound CD73 in inflammation. Front Immunol 2019;10:1729.

[28] Hashimoto M, Hossain S, Tanabe Y, Shido O. Effects of aging on the relation of adenyl purine release with plasma membrane fluidity of arterial endothelial cells. Prostaglandins Leukot Essent Fatty Acids 2005;73(6):475–83.

[29] Thom VT, Wendel M, Deussen A. Regulation of ecto-5 -nucleotidase by docosahexaenoic acid in human endothelial cells. Cell Physiol Biochem 2013;32(2):355–66.

[30] Webb G, Chen Y-Y, Li K-K, Neil D, Oo YH, Richter A, et al. Single-gene association between GATA-2 and autoimmune hepatitis: a novel genetic insight highlighting immunologic pathways to disease. J Hepatol 2016;64(5):1190–3.

[31] Borsellino G, Kleinewietfeld M, Di Mitri D, Sternjak A, Diamantini A, Giometto R, et al. Expression of ectonucleotidase CD39 by Foxp3+ Treg cells: hydrolysis of extracellular ATP and immune suppression. Blood 2007;110(4):1225–32.

[32] Dwyer KM, Hanidziar D, Putheti P, Hill PA, Pommey S, McRae JL, et al. Expression of CD39 by human peripheral blood CD4+CD25+ T cells denotes a regulatory memory phenotype. Am J Transplant 2010;10(11):2410–20.

[33] Vuerich M, Harshe R, Frank LA, Mukherjee S, Gromova B, Csizmadia E, et al. Altered aryl-hydrocarbon-receptor signalling affects regulatory and effector cell immunity in autoimmune hepatitis. J Hepatol 2021;74(1):48–57.

[34] Sauer AV, Brigida I, Carriglio N, Jofra Hernandez R, Scaramuzza S, Clavenna D, et al. Alterations in the adenosine metabolism and CD39/CD73 adenosinergic machinery cause loss of Treg cell function and autoimmunity in ADA-deficient SCID. Blood 2012;119(6):1428–39.

[35] Mihaylova MM, Shaw RJ. The AMPK signalling pathway coordinates cell growth, autophagy and metabolism. Nat Cell Biol 2011;13(9):1016–23.
[36] Yamaguchi H, Maruyama T, Urade Y, Nagata S. Immunosuppression via adenosine receptor activation by adenosine monophosphate released from apoptotic cells. eLife 2014;3.
[37] Hua Y, Liu D, Zhang D, Wang X, Wei Q, Qin W. Extracellular AMP suppresses endotoxemia-induced inflammation by alleviating neutrophil activation. Front Immunol 2020;11:1220.
[38] Butler JJ, Mader JS, Watson CL, Zhang H, Blay J, Hoskin DW. Adenosine inhibits activation-induced T cell expression of CD2 and CD28 co-stimulatory molecules: role of interleukin-2 and cyclic AMP signaling pathways. J Cell Biochem 2003;89(5):975–91.
[39] Bao R, Hou J, Li Y, Bian J, Deng X, Zhu X, et al. Adenosine promotes Foxp3 expression in Treg cells in sepsis model by activating JNK/AP-1 pathway. Am J Transl Res 2016;8(5):2284–92.
[40] Antonioli L, Pacher P, Vizi ES, Haskó G. CD39 and CD73 in immunity and inflammation. Trends Mol Med 2013;19(6):355–67.
[41] Mikhailov A, Sokolovskaya A, Yegutkin GG, Amdahl H, West A, Yagita H, et al. CD73 participates in cellular multiresistance Program and protects against TRAIL-induced apoptosis. J Immunol 2008;181(1):464–75.
[42] Alcedo KP, Rouse MA, Jung GS, Fu D, Minor M, Willcockson HH, et al. CD73 maintains hepatocyte metabolic integrity and mouse liver homeostasis in a sex-dependent manner. Cell Mol Gastroenterol Hepatol 2021;12(1):141–57.

